放疗专题 ·国际交流·

导读

自适应放疗(adaptive radiotherapy, ART)是图像引导精确放疗发展延伸出的一种放疗技术。治疗过程中,肿瘤和正常器官的位置及关系发生变化。ART 通过照射方式的改变来实现对患者组织解剖或肿瘤变化的调整,指导后续放疗计划的重新设计。ART 的实施分为在线和离线两种方式,它将最大限度地减少正常组织受量,进一步提高肿瘤放疗的精确性。该综述的作者作为国际 ART 的放射物理专家,立足于肺癌离线 ART 的进展,在技术发展、靶区勾画、变形配准、剂量累积、质量保证和临床运用等方面进行了详细评述,对临床有着重大意义。

冯 梅
四川省肿瘤医院 放疗中心

Adaptive Radiotherapy for Lung Cancer

Hualiang Zhong, X. Allen Li
Department of Radiation Oncology, Medical College of Wisconsin, Milwaukee, Wisconsin, USA
Corresponding author: X. Allen Li, Ph. D, E-mail: ali@ mcw. edu

[**Abstract**] The concept of adaptive radiotherapy (ART) was proposed 20 years ago, and since then a variety of methodologies and techniques have been developed to accommodate different clinical requirements, including both online and offline plan adaptations. Compared with pre-treatment planning, plan adaptation involves more computational tasks and consequently has increased complexity and computational burden. While ART can benefit many cancer patients, challenges still exist in development and implementation of high-quality ART programs. In this short review, we will focus on the development of offline ART for lung cancer. We will also discuss the advantages and disadvantages of different clinical implementations of ART.

[**Key words**] Adaptive radiotherapy; Lung cancer; Plan adaptation
Received November 4, 2018
Accepted December 4, 2018
doi:10.3969/j. issn. 1674-0904. 2019. 01. 002

Cite this article as: Zhong HL, Li XA. Adaptive radiotherapy for lung cancer [J]. J Cancer Control Treat, 2019, 32(1):7-16.

INTRODUCTION

Adaptive Radiation Therapy (ART) is a state-of-the-art approach that uses a treatment feedback process to account for patient-specific anatomic and/or biological changes, thus, delivering highly individualized radiation therapy for cancer patients [1]. ART strategies include offline and online adaptations. Offline ART generates a new radiation treatment (RT) plan based on the images acquired during the RT delivery session, accounting for information from previous treatment fractions, and delivers the new plan for subsequent fractions to correct for systematic variations [2]. In contrast, online ART generates a new plan based on the image of the day and delivers the new plan for that day's fraction accounting for both random and systematic changes [3-4]. This work will review technical aspects of offline ART based on its applications for lung cancer.

It has been well documented that advanced RT technologies have significantly improved radiation treatment outcome for lung cancer. For example, a large population-based study showed that IMRT improves overall survival for patients with T3 and T4 tumors [5]. Another example is on-board imaging (OBI) which helps reduce patient setup errors and minimize radiation toxicity to surrounding normal tissue. With the assis-

tance of OBI, stereotactic body radiotherapy (SBRT) has significantly improved clinical outcomes [6-9]. The emergence of MRI-Linac may further enhance the capabilities of real-time tracking for intra-fractional tumor motion, and online plan adaptation could consequently be achieved by making radiation beams conformal to tumor targets throughout the whole treatment course [4,10-11].

Different from lung SBRT which has been reported to be an efficient treatment modality, dose escalation for locally advanced cancer patients has not yet been implemented in clinic because escalating target dose may result in the increased risk of normal tissue complications [12-14]. On the other hand, tumor volumes may change during the course of treatment. For example, with 1.2% daily tumor regression as reported in literature, the pre-treatment plan can be adapted with beams conformal to reduced tumor targets. This may help increase target dose, reduce normal tissue toxicity, and thereby improve treatment outcomes for these patients [15-17]. These pre-clinical studies have highlighted the importance of clinical implementation of adaptive radiotherapy. Since ART involves many techniques and can be applied to different clinical scenarios, it is not feasible to introduce all the aspects of this treatment modality in a short review. Instead, this article will go through the major technical components developed for off-line plan adaption for patients with locally advanced lung cancer.

TECHNICAL DEVELOPMENT

ART involves many tasks such as developing an initial treatment plan, evaluating treatment response using computed tomography (CT), cone beam computed tomography (CBCT) or positron emission tomography (PET) images, and making decisions on plan adaptation. If required, an adaptive plan will be developed that includes re-contouring, dose accumulation, plan re-optimization, and quality assurance. In the following sections we will discuss the current status of technical development for each of these tasks.

Contour re-generation

Contour delineation for tumor targets and organs at risk is a time-consuming process in treatment planning[18]. While frequent plan adaptations may help maximize the benefits of ART [19], transitional gains in each adaptation step may be counteracted by tremendous efforts put in re-contouring and other re-planning tasks. To address this issue, different approaches were developed to automatically generate contours. Various 2D or 3D auto-segmentation techniques such as region-growing and "snake" algorithms have been developed for direct segmentation of different anatomic structures such as bone, pancreas, heart, esophagus [20-21]; deformable image registration (DIR) algorithms have also been employed to automatically propagate contours from the original planning CT images to during-RT images [22-23]. Due to limited contrasts and gradients in during-RT images, the registrations could have large errors, and the propagated volumes need to be thoroughly assessed [9].

Atlas-based segmentation methods are expected to segment image structures that have no obvious intensity differences, where the *a priori* information about the difference between these objects can be incorporated in spatial relationship or statistical models [24]. Recent developments in machine learning have revolutionized the field of artificial intelligence. Deep learning algorithms, especially deep convolutional neural networks (DCNN), are a powerful methodology for solving challenging medical imaging problems such as tumor detection, disease classification, and structure segmentation [25]. Different atlas-based segmentation approaches could consequently be enhanced by the developed machine learning techniques [26].

Deformable image registration (DIR)

Deformable registration of two images is to establish a correspondence map that matches anatomical structures in one image to their counterparts in the other image. The counterparts could be the same structures appeared in the two images acquired at different times or with different modalities. In adaptive radiotherapy, longitudinal images are often acquired at different treatment stages for treatment planning, patient setup, tumor localization, or treatment response assessment. To use these images correctly, the acquired images need to be registered to a reference image such that information contained in these images can be appropriately interpreted or assessed. DIR is a key component in

development of adaptive radiotherapy techniques and is required almost at every step in the process of plan adaptation. Except the contour propagation mentioned before, dose accumulation, 4D planning and treatment response assessment all require accurate DIR. Development of an appropriate DIR algorithm for each of these subjects is an active area of research.

Over the last two decades many registration algorithms have been developed, among which the optical flow-based "demons" and B-spline-based free form are two major algorithms developed in many free and commercial software packages [27-28]. These algorithms have been modified or improved over the years for different applications. For example, Yang et al generated inverse consistent DVFs to improve the accuracy of the demons registration [29] and Vercauteren et al made the underlying transformation diffeomorphic to generate more smooth deformation fields [30-31]; Rueckert et al made the parametric B-spline-based registration algorithm diffeomorphic [32], which was then extended to be hierarchical [33] and to have non-uniform knot placements [34] and simplified regularizations [35]. The B-Spline and demons algorithms could be combined with a mechanical model-based finite element method (FEM) to register anatomical structures in the case of large-scale deformation [36-37]. These methods were extended to registration of soft tissue in low contrast regions [38] and between different modality images [39]. The mechanical model-based hybrid registrations could also reduce registration errors in the neighborhood of regressing tumors (Figure 1), and meanwhile maintain the integrity of dose mapping [39-40]. These technical developments have enhanced the efficiency of structure contouring and dose accumulation and improved the quality of adaptive radiotherapy[9, 41-42].

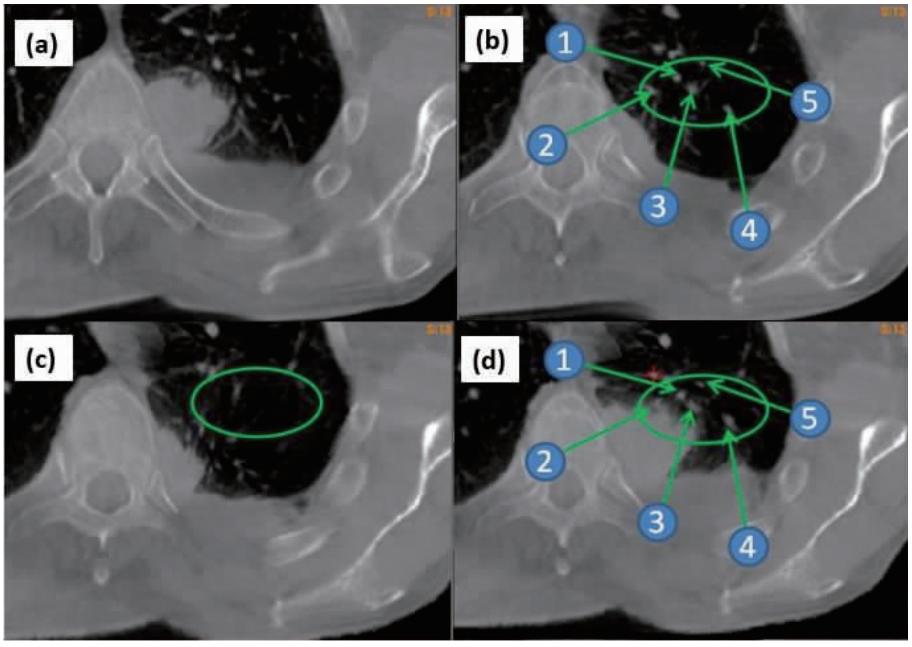

Figure 1. CBCT Images

CBCT images acquired at fraction 1 and 25 shown in (a) and (b), respectively; (c) the warped source image (fraction 1) using VelocityAI, and (d) the warped source image using the FEM-based hybrid method, resulting in landmarks consistent to their positions at fraction 25.

It should be mentioned that computational time for DIR currently is not yet sufficient for online ART. The computation speed may depend on multiple factors such as image size, parametric resolution and number of iterations implemented in these algorithms, and simplifying these parameters may compromise the accuracy of deformable registration [43]. To address these issues, Gu et al demonstrated that the GPU-enhanced demons algorithm could complete 4D-CT image registrations around 10 seconds [44]. In contrast, while B-spline-based registration algorithms are capable of performing both unimodal and multimodal registrations, it is difficult to improve the speed of these algorithms due to their computational complexity.

Accumulation of delivered doses

To develop an adaptive plan for the remaining treatment fractions, radiation dose delivered up-to-date needs to be accumulated in each image voxel. The accuracy of dose accumulation depends on dose mapping and its underlying DIR methods used. Most registration algorithms could currently be accurate within 2 ~ 3 mm on average [43, 45-46] which is comparable to the resolution of dose grids often used in clinic [47-48], while some algorithms could have the mean error up to 6.9 mm [46]. The registration errors may induce dose mapping uncertainties up to 3 Gy/mm [49], and the clinical impact of the spatial errors may need further investigations [50].

With a correct registration map, dose delivered at each fraction could be mapped to a reference image and summated to get the total dose. However, dose interpolation methods may induce dose mapping errors in regions with high dose gradients, and some large errors even not at a steep dose gradient [51]. The latter could be due to different formations of image grids between the source and target images. Deformable dose accumulation (DDA) could also be compromised by changes in the mass and volume of solid tumors and/or normal tissue over the course of treatment. To address these issues, 4D Monte Carlo-based methods such as voxel-warping method (VWM) [52], energy-mass congruent mapping (EMCM) [53] and energy-conserved registration methods [39, 54] were proposed to help improve the quality of dose accumulation. Recently EMCM was applied to model-based dose calculation algorithms in a commercial software package [39-40], and its computation speed was improved significantly by using a GPU-based computational approach [55].

Quality assurance

Adaptive treatment planning involves 3D dose calculation, DIR, contour propagation, dose warping and accumulation. Ideally each of these tasks could be evaluated separately for each patient. Different from conventional dose calculation algorithms which can be verified with homogeneous and heterogeneous dosimetric phantoms, the total dose delivered to deforming organs over the course of treatment is difficult to verify. This is mainly due to the lack of a gold standard required to evaluate the DIR and DDA operations [56]. It is necessary to have independent verifications of dose accumulation for each patient. In general, two kinds of verifications can be performed.

Spatial accuracy: landmark and contour consistencies and DICE similarity coefficients are often used as criteria to evaluate the performance of DIR in different applications [46, 57-59], and the self and inverse consistencies of deformation maps have also been used to evaluate the accuracy of the registration [29, 60-61]; computational phantoms offer another option to verify the accuracy of displacements at all voxels in the registered images. The phantom's deformation can be simulated using different mathematical formulae [62]. With the aid of the finite element method, Stanley et al created a patient-specific deformable model to improve the realism of tissue deformation for a lung cancer patient [63]. The FEM-computed deformable model and a deformable dosimetry were overlaid as shown in Figure 2 (a).

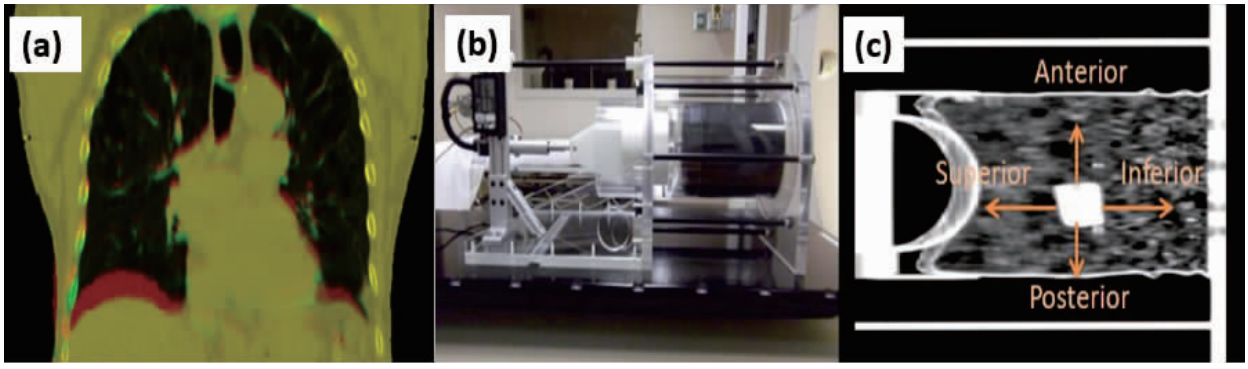

Figure 2. The FEM-computed Deformable Model and a Deformable Dosimetry

(a) A lung patient CT image overlaid on its warped image using a patient-specific FEM model; (b) a deformable dosimetry phantom; (c) the CT image of the dosimetry phantom.

Dosimetry accuracy: different from computational phantoms, physical phantoms may help measure the delivered dose to verify dose accumulation operations. Figure 2 (b) showed a deformable phantom containing heterogeneous sponges for simulating respiratory motion. The phantom with deformation automatically driven by a motor was irradiated, and delivered doses were measured by imbedded thermoluminescent dosimeters (TLDs). However, these phantoms are unable to simulate mass changes in tumors and other organs while these changes are often observed during the course of treatment. Also these phantoms do not show realistic organ deformation and mass heterogeneity as patients, so further improvement of these phantoms is highly desired [64-66]. It was suggested that the phantom-based evaluations should be supplemented by other verification methods such as the energy conservation criterion that can be applied to both deformed anatomical structures and regressed tumor volumes [39, 54].

CLINICAL IMPLEMENTATION

When patients have large spatial changes in tumor targets or organs at risk, it is important to have the initial treatment plan adapted. Different adaptive planning strategies, however, could result in different clinical outcomes.

Applications of adaptive radiotherapy

As the PTV is generally large for locally advanced non-small-cell lung carcinoma (NSCLC), the initial treatment plan often show high radiation dose to healthy tissue. For example, the treatment regimen of 30 × 2 Gy to tumor targets may cause mean lung dose (MLD) to exceed 20 Gy for patients with bulky tumors. On the other hand, it was observed that lung tumors regress of about 50% volume over the course of fractionated RT [16-17, 67-69]. For these patients, radiation beams could be reshaped to the residual tumor target after delivering a number of treatment fractions, and this may reduce radiation toxicity to surrounding tissue.

Radiation therapy with the radiation target field updated during the course of treatment has recognized potential to benefit patients (the NRG/RTOG Trial No. 1106) [70-72]. It was reported that escalating radiation dose may help improve tumor locoregional control and overall survival [73-74]. With tumor regression, high-quality ART may ensure iso-toxic dose escalation which may consequently help improve clinical outcomes [75-77].

In addition, radiation treatment may change anatomical structures and physiological functions. For example, airway obstruction could be alleviated after a few weeks of treatment. This will allow the collapsed lung structures re-ventilated. Respiratory patterns could consequently change and the relative positions of lung and other structures could be different after the treatment. The atelectatic changes combined with anatomical variations may render it necessary to update the pretreatment plan for the remaining treatment fractions [68].

Frequency of plan adaptation

As tumor continuously shrinks during the course of treatment, there is a trade-off between the amount of the reduced tumor volume and the number of the remaining fractions [69]. It has been reported that plan adaptation performed around fraction 15 and fraction 20 is most dosimetrically efficient for concurrent and sequential chemo-radiotherapy, respectively. Based on iso-toxic mean lung dose (MLD), re-planning twice at weeks 2 and 4 may achieve an average escalation of 13.4 Gy [71], and at weeks 3 and 5 may have an average increase of 7 Gy on tumor targets. Since tumor shrinkage depends on many factors such as tumor histology, location, stage and imaging modality used in the volume measurement, the optimal time point for plan adaptation and its dosimetric gain could have variations for individual patients.

The benefits of adaptive planning in terms of normal tissue sparing have also been investigated by multiple investigators. Guckenberger et al showed that when the GTV volume reduced 39% on average, a single plan adaptation at the end of week 4 was able to reduce MLD by 100 cGy on average [19, 77]. Dial et al demonstrated that the mid-treatment plan adaptation reduced MLD by 38 cGy for patients having an average GTV reduction of 21% at the end of the treatment [19]; Woodford et al found that the MLD reductions are in the range of 30 to 160 cGy for three patients [78]. These results suggested that the majority of the gains from ART can be achieved by implementing a single mid-treatment adaptation if the tumor volume regresses by 30%

within the first 20 fractions [78].

It should be mentioned that large uncertainties may exist in the measurement of residual tumor volumes. For example, internal hemorrhage, necrosis, or metabolically non-viable tumor cells could be mis-counted in the measured volume, especially when only CBCT images were used for the volume measurement [17]. Compared to CT or CBCT images, FDG-PET images can show metabolic activities in addition to the tumor volume. It was therefore recommended that both CT and PET images shall be used for the mid-treatment tumor response measurement for adaptive RT [70,79]. Note that the standardized uptake value (SUV) of PET images could be influenced by many factors [80-82], and changes in region-specific SUVs cannot be quantified until the correspondent images are correctly registered [82-84]. While the Response Evaluation Criteria in Solid Tumors (RECIST) has been used as a criterion for evaluation of tumor response in clinic [85], methods for quantitative assessments of tumor response, in addition to tumor volume measurements, are worth further investigations.

Dose regimens for adaptive planning

It has been reported that for locally advanced NSCLC, dose regimens in the range of 60 ~ 66 Gy have 5-year overall survival rates at 10% ~ 15% [86]. Although a randomized trial did not show superiority at a dose of 74 Gy [14], the reasons for the underperformance of the higher dose arm are still unclear [87-89]. Technical factors such as respiratory motion management, treatment planning margin, delivery mode (IMRT *vs* 3D-CRT) and imaging modality used for treatment planning and delivery all could have impacts on the clinical outcomes, and each of these components may be worth further investigations [87,90]. It was reported that for patients with locally advanced NSCLC, adaptive planning increases radiation dose up to 80 Gy on average on the residual tumor without increasing MLD [68,71]. In general, improved treatment planning and delivery techniques will help better spare lung, heart and other healthy organs from irradiation [86].

For lung cancer patients, it has been reported that increasing dose from 60 Gy to 74 Gy results in predictable, deleterious effects on quality of life [91]. For these patients, RT-induced adverse events may include pneumonitis, esophagitis and pericarditis [92], and therefore radiation dose to these organs should be minimized. Compared to dose escalation, it is of equivalent importance to develop effective treatment strategies to mitigate normal tissue toxic effects for these patients. It was shown that for iso-prescription adaptive plans (relative to initial plans), mean lung dose was reduced, on average from 17.3 Gy (initial plan) to 14.8 Gy for the adapted plans [68,71]. It is worth conducting clinical trials to compare clinical gains of different ART strategies, e. g.: iso-toxic dose escalation *vs* iso-prescription, for plan adaptation. It has been reported, recently, from a phase 2 clinical trial that PET-CT guided ART for locally advanced NSCLC improved local-regional control [93]. With more clinical data being collected on locoregional control and overall survival, it will be possible to develop optimized dose regimens and treatment protocols for ART.

DISCUSSION

Since patients with locally advanced NSCLC often have tumor regression during the course of fractionated radiotherapy, updating their initial RT plan may help enable dose escalation to residual tumor targets and spare normal tissue. Pre-clinical studies have shown a great promise for adaptive radiotherapy to treat these patients. Different strategies such as iso-toxic target dose escalation or iso-prescription normal tissue sparing have been proposed for plan adaptation. The emergency of onboard imaging, especially MRI-Linac, has rendered ART an imperative treatment modality for many patients. While significant progress has been made in the past twenty years for automatic contouring, image registration, dose accumulation and re-planning algorithms, ART techniques remain to be improved before they can be routinely used for treatment of NSCLC patients [94].

Since DIR plays multiple roles in ART, registration accuracy is still the major concern for the clinical implementation of ART. It has been illustrated that intensity-based DIR algorithms are prone to have errors in regions with low image contrasts [43,45,95], and tumor regression may also cause registration errors in nearby

normal tissue. For every 10% regression in tumor volume, the dose error associated with a rigid (non-deformable) registration algorithm for computing accumulated dose is approximately 1 Gy [68]. The large dose errors (up to 5 ~ 6 Gy for 50% tumor regression) will downgrade the quality of adaptive therapy and are likely to impact treatment outcomes [56]. Due to the lack of knowledge on the pattern of tumor regression, how to deform the anatomical structures nearby the tumor is still unclear [68,72]. While mechanical models have been introduced to improve registration accuracy, their parameters and constraints still need to be optimized. Since registration errors could be propagated to dose reconstruction and response assessment, the accuracy of these algorithms in clinical settings needs to be further evaluated. Also with DIR used in more clinical applications, computational speeds for FEM or B-Spline-based registrations need to be improved.

Different from development of an initial treatment plan, CTV margins required for an adaptive plan could depend on the precision and efficiency of delivered treatment. Since tumor response is not uniform, survived tumor cells may exist sporadically. Similar to sub-clinical disease spread from initial gross tumor volumes, tumor cells may survive in the regions surrounding the residual tumor, and these regions still need to be covered by an updated CTV for the adaptive plan [96]. While PET images, after appropriate registrations, may help identify regions with high metabolic activities, the resolution of these images is limited, and the survived tumor cells cannot be detected effectively. Since treatment efficacy is patient dependent, it is not straightforward to find the optimal dose required to eliminate the remaining tumor cells.

Adaptive planning strategies, with different dose levels assigned to the remaining tumor and to the regions with subclinical diseases, respectively, have been considered in clinical trials [90]. Different from the sub-volume boosting to each segment in these trials, dose painting has also been proposed by using a voxel-level dose prescription based on image intensity changes in individual pixels [97]. The quantitative use of images, termed as theragnostic imaging, may help determine the minimal radiation dose required to treat individual patients. When image quantities are directly associated with radiation dose, the quality of these images and their derivatives should be reviewed with high standard criteria.

Pre-clinical studies have shown that ART may help optimize treatment regimens, improve clinical outcomes, and consequently benefit many cancer patients. It is worth improving adaptive planning techniques and meanwhile investigating the efficacy of different ART strategies with more clinical trials.

REFERENCES

[1] Li XA. Adaptive Radiation Therapy [M]. Hendee WR, editor. Boca Raton: CRC Press; 2011.

[2] Yan D, Vicini F, Wong J, et al. Adaptive radiation therapy [J]. Phys Med Biol, 1997, 42(1): 123 - 132.

[3] Ahunbay EE, Peng C, Chen GP, et al. An on-line replanning scheme for interfractional variations [J]. Med Phys. 2008, 35(8): 3607-3615.

[4] Klawikowski S, Tai A, Ates O, et al. A fast 4D IMRT/VMAT planning method based on segment aperture morphing [J]. Med Phys, 2018, 45(4): 1594-1602.

[5] Jegadeesh N, Liu Y, Gillespie T, et al. Evaluating intensity-modulated radiation therapy in locally advanced non-small-cell lung cancer: results from the National Cancer Data Base. Clin Lung Cancer, 2016, 17(5): 398-405.

[6] Rosenzweig KE, Fox JL, Yorke E, et al. Results of a phase I dose-escalation study using three-dimensional conformal radiotherapy in the treatment of inoperable nonsmall cell lung carcinoma [J]. Cancer, 2005, 103(10): 2118-2127.

[7] Bezjak A, Papiez L, Bradley JD, et al. RTOG 0813 Protocol: Seamless Phase I/II Study of Stereotactic Lung Radiotherapy (SBRT) for Early Stage, Centrally Located, Non-Small Cell Lung Cancer (NSCLC) in Medically Inoperable Patients[EB/OL]. http://www. rtogorg/ClinicalTrials/ProtocolTable/StudyDetailsaspx?study = 0813. 2012.

[8] Matsuo Y, Chen F, Hamaji M, et al. Comparison of long-term survival outcomes between stereotactic body radiotherapy and sublobar resection for stage I non-small-cell lung cancer in patients at high risk for lobectomy: A propensity score matching analysis [J]. Eur J Cancer, 2014, 50(17): 2932-2938.

[9] Hardcastle N, van Elmpt W, De Ruysscher D, et al. Accuracy of deformable image registration for contour propagation in adaptive lung radiotherapy [J]. Radiat Oncol, 2013, 18(8): 243.

[10] Al-Ward SM, Kim A, McCann C, et al. The development of a 4D treatment planning methodology to simulate the tracking of central lung tumors in an MRI-linac [J]. J Appl Clin Med Phys, 2018, 19(1): 145-155.

[11] Ge Y, O'Brien RT, Shieh CC, et al. Toward the development of intrafraction tumor deformation tracking using a dynamic multi-leaf

collimator [J]. Med Phys, 2014, 41(6): 061703.

[12] Movsas B, Raffin TA, Epstein AH, et al. Pulmonary radiation injury [J]. Chest, 1997, 111(4): 1061-176.

[13] Yamashita H, Takahashi W, Haga A, et al. Radiation pneumonitis after stereotactic radiation therapy for lung cancer [J]. World J Radiol, 2014, 6(9): 708-715.

[14] Bradley JD, Moughan J, Graham MV, et al. A phase I/II radiation dose escalation study with concurrent chemotherapy for patients with inoperable stages I to III non-small-cell lung cancer: phase I results of RTOG 0117 [J]. Int J Radiat Oncol Biol Phys, 2010, 77(2): 367-372.

[15] Kong FM, Ritter T, Quint DJ, et al. Consideration of dose limits for organs at risk of thoracic radiotherapy: atlas for lung, proximal bronchial tree, esophagus, spinal cord, ribs, and brachial plexus [J]. Int J Radiat Oncol Biol Phys, 2011, 81(5): 1442-1457.

[16] Kupelian PA, Ramsey C, Meeks SL, et al. Serial megavoltage CT imaging during external beam radiotherapy for non-small-cell lung cancer: observations on tumor regression during treatment [J]. Int J Radiat Oncol Biol Phys, 2005, 63(4): 1024-1028.

[17] Lim G, Bezjak A, Higgins J, et al. Tumor regression and positional changes in non-small cell lung cancer during radical radiotherapy [J]. J Thorac Oncol, 2011, 6(3): 531-536.

[18] Kumarasiri A, Siddiqui F, Liu C, et al. Deformable image registration based automatic CT-to-CT contour propagation for head and neck adaptive radiotherapy in the routine clinical setting [J]. Med Phys, 2014, 41(12): 121712.

[19] Dial C, Weiss E, Siebers JV, et al. Benefits of adaptive radiation therapy in lung cancer as a function of replanning frequency [J]. Med Phys, 2016, 43(4): 1787.

[20] Tan S, Li L, Choi W, et al. Adaptive region-growing with maximum curvature strategy for tumor segmentation in (18)F-FDG PET [J]. Phys Med Biol, 2017, 62(13): 5383-5402.

[21] Kiaei AA, Khotanlou H. Segmentation of medical images using mean value guided contour [J]. Med Image Anal, 2017, 40: 111-132.

[22] Lu W, Olivera GH, Chen Q, et al. Automatic re-contouring in 4D radiotherapy [J]. Phys Med Biol, 2006, 51(5): 1077-1099.

[23] Shekhar R, Lei P, Castro-Pareja CR, et al. Automatic segmentation of phase-correlated CT scans through nonrigid image registration using geometrically regularized free-form deformation [J]. Med Phys, 2007, 34(7): 3054-3066.

[24] Daisne JF, Blumhofer A. Atlas-based automatic segmentation of head and neck organs at risk and nodal target volumes: a clinical validation [J]. Radiat Oncol, 2013, 8: 154.

[25] Xu J, Luo X, Wang G, et al. A Deep Convolutional Neural Network for segmenting and classifying epithelial and stromal regions in histopathological images [J]. Neurocomputing. 2016, 191: 214-223.

[26] Sdika M. Enhancing atlas based segmentation with multiclass linear classifiers [J]. Med Phys, 2015, 42(12): 7169-7181.

[27] Thirion JP. Image matching as a diffusion process: an analogy with Maxwell's demons [J]. Med Image Anal, 1998, 2(3): 243-260.

[28] Rueckert D, Sonoda LI, Hayes C, et al. Nonrigid registration using free-form deformations: application to breast MR images [J]. IEEE Trans Med Imaging, 1999, 18(8): 712-721.

[29] Yang D, Li H, Low DA, et al. A fast inverse consistent deformable image registration method based on symmetric optical flow computation [J]. Phys Med Biol, 2008, 53(21): 6143-6165.

[30] Vercauteren T, Pennec X, Perchant A, et al. Diffeomorphic demons: efficient non-parametric image registration [J]. Neuro Image, 2009, 45(S1): S61-S72.

[31] Yeo BT, Sabuncu MR, Vercauteren T, et al. Spherical demons: fast diffeomorphic landmark-free surface registration [J]. IEEE Trans Med Imaging, 2010, 29(3): 650-668.

[32] Rueckert D, Aljabar P, Heckemann RA, et al. Diffeomorphic registration using B-splines [J]. Med Image Comput Comput Assist Interv, 2006, 9(2): 702-709.

[33] Klein S, Staring M, Murphy K, et al. Elastix: a toolbox for intensity-based medical image registration [J]. IEEE Trans Med Imaging, 2010, 29(1): 196-205.

[34] Jacobson TJ, Murphy MJ. Optimized knot placement for B-splines in deformable image registration [J]. Med Phys, 2011, 38(8): 4579-4582.

[35] Chun SY, Fessler JA. A simple regularizer for B-spline nonrigid image registration that encourages local invertibility [J]. IEEE J Sel Top Signal Process, 2009, 3(1): 159-169.

[36] Zhong H, Cai J, Glide-Hurst C, et al. An adaptive finite element method to cope with a large scale lung deformation in magnetic resonance images[A]. 2014 IEEE 11th International Symposium on Biomedical Imaging (ISBI)[C]. IEEE: 770-773, 2014.

[37] Huang X, Ren J, Abdalbari A, et al. Deformable image registration for tissues with large displacements [J]. J Med Imaging, 2017, 4(1): 014001.

[38] Zhong H, Kim J, Li H, et al. A finite element method to correct deformable image registration errors in low-contrast regions [J]. Phys Med Biol, 2012, 57(11): 3499-3515.

[39] Zhong H, Chetty IJ. Adaptive radiotherapy for NSCLC patients: utilizing the principle of energy conservation to evaluate dose mapping operations [J]. Phys Med Biol, 2017, 62(11): 4333-4345.

[40] Li HS, Zhong H, Kim J, et al. Direct dose mapping versus energy/mass transfer mapping for 4D dose accumulation: fundamental differences and dosimetric consequences [J]. Phys Med Biol, 2014, 59(1): 173-188.

[41] Chao M, Schreibmann E, Li T, et al. Automated contour mapping using sparse volume sampling for 4D radiation therapy[J]. Med-Phys, 2007, 34(10): 4023-4029.

[42] Mencarelli A, van Kranen SR, Hamming-Vrieze O, et al. Deformable image registration for adaptive radiation therapy of head and neck cancer: accuracy and precision in the presence of tumor changes [J]. Int J Radiat Oncol Biol Phys, 2014, 90(3): 8.

[43] Zhong H, Kim J, Chetty IJ. Analysis of deformable image registration accuracy using computational modeling [J]. Med Phys, 2010, 37(3): 970-979.

[44] Gu X, Pan H, Liang Y, et al. Implementation and evaluation of various demons deformable image registration algorithms on a GPU [J]. Phys Med Biol, 2010, 55(1): 207-219.

[45] Yeo UJ, Supple JR, Taylor ML, et al. Performance of 12 DIR algorithms in low-contrast regions for mass and density conserving deformation [J]. Med Phys, 2013, 40(10): 101701.

[46] Castillo R, Castillo E, Guerra R, et al. A framework for evaluation of deformable image registration spatial accuracy using large landmark point sets [J]. Phys Med Biol, 2009, 54(7): 1849-1870.

[47] Rosu M, Chetty IJ, Balter JM, et al. Dose reconstruction in deforming lung anatomy: dose grid size effects and clinical implications [J]. Med Phys, 2005, 32(8): 2487-2495.

[48] Park JY, Kim S, Park HJ, et al. Optimal set of grid size and angular increment for practical dose calculation using the dynamic conformal arc technique: a systematic evaluation of the dosimetric effects in lung stereotactic body radiation therapy [J]. Radiat Oncolog, 2014, 9: 5.

[49] Salguero FJ, Saleh-Sayah NK, Yan C, et al. Estimation of three-dimensional intrinsic dosimetric uncertainties resulting from using deformable image registration for dose mapping [J]. Med Phys, 2011, 38(1): 343-353.

[50] Roussakis YG, Dehghani H, Green S, et al. Validation of a dose warping algorithm using clinically realistic scenarios [J]. Br J Radiol, 2015, 88(1049): 20140691.

[51] Siebers JV, Zhong H. An energy transfer method for 4D Monte Carlo dose calculation [J]. Med Phys, 2008, 35(9): 4096-4105.

[52] Heath E, Seuntjens J. A direct voxel tracking method for four-dimensional Monte Carlo dose calculations in deforming anatomy [J]. Med Phys, 2006, 33(2): 434-445.

[53] Zhong H, Siebers JV. Monte Carlo dose mapping on deforming anatomy [J]. Phys Med Biol, 2009, 54(19): 5815-5830.

[54] Zhong H, Chetty IJ. Caution must be exercised when performing deformable dose accumulation for tumors undergoing mass changes during fractionated radiation therapy [J]. Int J Radiat Oncol Biol Phys, 2017, 97(1): 182-183.

[55] Ziegenhein P, Kamerling CP, Fast MF, et al. Real-time energy/mass transfer mapping for online 4D dose reconstruction [J]. Sci Rep, 2018, 8(1): 3662.

[56] Jaffray DA, Lindsay PE, Brock KK, et al. Accurate accumulation of dose for improved understanding of radiation effects in normal tissue [J]. Int J Radiat Oncol Biol Phys, 2010, 76(S3): S135-S139.

[57] Kaus MR, Brock KK, Pekar V, et al. Assessment of a model-based deformable image registration approach for radiation therapy planning [J]. Int J Radiat Oncol Biol Phys, 2007, 68(2): 572-580.

[58] Lu W, Chen ML, Olivera GH, et al. Fast free-form deformable registration via calculus of variations [J]. Phys Med Biol, 2004, 49(14): 3067-3087.

[59] Kim J, Hammoud R, Pradhan D, et al. Prostate localization on daily cone-beam computed tomography images: accuracy assessment of similarity metrics [J]. Int J Radiat Oncol Biol Phys, 2010, 77(4): 1257-1265.

[60] Christensen GE, Johnson HJ. Consistent image registration [J]. IEEE Trans Med Imaging, 2001, 20(7): 568-582.

[61] Zhong H, Peters T, Siebers JV. FEM-based evaluation of deformable image registration for radiation therapy [J]. Phys Med Biol, 2007, 52(16): 4721-4738.

[62] Wang H, Dong L, O'Daniel J, et al. Validation of an accelerated 'demons' algorithm for deformable image registration in radiation therapy [J]. Phys Med Biol, 2005, 50(12): 2887-2905.

[63] Stanley N, Glide-Hurst C, Kim J, et al. Using patient-specific phantoms to evaluate deformable image registration algorithms for adaptive radiation therapy [J]. J Appl Clin Med Phys, 2013, 14(6): 6.

[64] Zhong H, Adams J, Glide-Hurst C, et al. Development of a deformable dosimetric phantom to verify dose accumulation algorithms for adaptive radiotherapy [J]. J Med Phys, 2016, 41(2): 106-114.

[65] Yeo UJ, Taylor ML, Supple JR, et al. Is it sensible to "deform" dose? 3D experimental validation of dose-warping [J]. Med Phys, 2012, 39(8): 5065-5072.

[66] Niu CJ, Foltz WD, Velec M, et al. A novel technique to enable experimental validation of deformable dose accumulation [J]. Med Phys, 2012, 39(2): 765-776.

[67] Guckenberger M, Richter A, Wilbert J, et al. Adaptive radiotherapy for locally advanced non-small-cell lung cancer does not underdose the microscopic disease and has the potential to increase tumor control [J]. Int J Radiat Oncol Biol Phys, 2011, 81(4): e275-e282.

[68] Zhong H, Siddiqui S, Movsas B, et al. Evaluation of adaptive treatment planning for patients with non-small cell lung cancer [J]. Phys Med Biol, 2017, 62(11): 4346-4360.

[69] Berkovic P, Paelinck L, Lievens Y, et al. Adaptive radiotherapy for locally advanced non-small cell lung cancer, can we predict when and for whom? [J]. Acta oncol, 2015, 54(9): 1438-1444.

[70] Kong FM, Machtay M, Bradley J, et al. RTOG 1106/ACRIN 6697: randomized phase II trial of individualized adaptive radiotherapy using during-treatment FDG-PET/CT and modern technology in locally advanced non-small cell lung cancer (NSCLC) [EB/OL]. https://clinicaltrials.gov/ct2/show/NCT01507428, 2013.

[71] Weiss E, Fatyga M, Wu Y, et al. Dose escalation for locally advanced lung cancer using adaptive radiation therapy with simultaneous integrated volume-adapted boost [J]. Int J Radiat Oncol Biol Phys, 2013, 86(3): 414-419.

[72] Sonke JJ, Belderbos J. Adaptive radiotherapy for lung cancer [J]. Semin Radiat Oncol, 2010, 20(2): 94-106.

[73] Jensen AD, Munter MW, Bischoff HG, et al. Combined treatment of nonsmall cell lung cancer NSCLC stage III with intensity-modulated RT radiotherapy and cetuximab: the NEAR trial [J]. Cancer, 2011, 117(13): 2986-2994.

[74] Rengan R, Rosenzweig KE, Venkatraman E, et al. Improved local control with higher doses of radiation in large-volume stage III non-small-cell lung cancer [J]. Int J Radiat Oncol Biol Phys, 2004, 60(3): 741-747.

[75] Brown JM, Carlson DJ, Brenner DJ. The tumor radiobiology of SRS and SBRT: are more than the 5 Rs involved? [J]. Int J Radiat Oncol Biol Phys, 2014, 88(2): 254-262.

[76] Kong FM, Ten Haken RK, Schipper MJ, et al. High-dose radiation improved local tumor control and overall survival in patients with inoperable/unresectable non-small-cell lung cancer : long-term results of a radiation dose escalation study [J]. Int J Radiat Oncol Biol Phys, 2005, 63(2):324-333.

[77] Guckenberger M, Wilbert J, Richter A, et al. Potential of adaptive radiotherapy to escalate the radiation dose in combined radiochemotherapy for locally advanced non-small cell lung cancer [J]. Int J Radiat Oncol Biol Phys, 2011, 79(3):901-908.

[78] Woodford C, Yartsev S, Dar AR, et al. Adaptive radiotherapy planning on decreasing gross tumor volumes as seen on megavoltage computed tomography images [J]. Int J Radiat Oncol Biol Phys, 2007, 69(4):1316-1322.

[79] Feng M, Kong FM, Gross M, et al. Using fluorodeoxyglucose positron emission tomography to assess tumor volume during radiotherapy for non-small-cell lung cancer and its potential impact on adaptive dose escalation and normal tissue sparing [J]. Int J Radiat Oncol Biol Phys, 2009, 73(4):1228-1234.

[80] Callahan J, Binns D, Dunn L, et al. Motion effects on SUV and lesion volume in 3D and 4D PET scanning [J]. Australas Phys Eng Sci Med, 2011, 34(4):489-495.

[81] Pan T, Mawlawi O, Nehmeh SA, et al. Attenuation correction of PET images with respiration-averaged CT images in PET/CT [J]. J Nucl Med, 2005, 46(9):1481-1487.

[82] Biehl KJ, Kong FM, Dehdashti F, et al. 18F-FDG PET definition of gross tumor volume for radiotherapy of non-small cell lung cancer : is a single standardized uptake value threshold approach appropriate? [J]. J Nucl Med, 2006, 47(11):1808-1812.

[83] Lu W, Wang J, Zhang HH. Computerized PET/CT image analysis in the evaluation of tumour response to therapy [J]. Br J Radiol, 2015, 88(1048):20140625.

[84] Zhong H, Brown S, Chetty I. Voxel-based tracking of 18F-FDG PET images for evaluation of treatment response for NSCLC patients [A]. AACR-NCI-EORTC International Conference on Molecular Targets and Cancer Therapeutics[C]. AACR, 2015. 1.

[85] Eisenhauer EA, Therasse P, Bogaerts J, et al. New response evaluation criteria in solid tumours : revised RECIST guideline (version 1.1) [J]. Eur J Cancer, 2009, 45(2):228-247.

[86] Kong FM, Zhao J, Wang J, et al. Radiation dose effect in locally advanced non-small cell lung cancer. Journal of thoracic disease [J]. 2014, 6(4):336-347.

[87] Kong FM, Haken RKT, Schipper M, et al. A phase II trial of mid-treatment FDG-PET adaptive, individualized radiation therapy plus concurrent chemotherapy in patients with non-small cell lung cancer (NSCLC) [J]. J Clin Oncol, 2013, 31(S1):7522.

[88] Cox JD. Are the results of RTOG 0617 mysterious? [J]. Int J Radiat Oncol Biol Phys, 2012, 82(3):1042-1044.

[89] Thomas CR, Jr. The importance of quality of life assessment [J]. JAMA Oncol, 2016, 2(3):367-368.

[90] Movsas B, Hu C, Sloan J, et al. Quality of life (QOL) analysis of the randomized radiation (RT) dose-escalation NSCLC trial (RTOG 0617) : The Rest of the Story [J]. Int J Radiat Oncol Biol Phys, 2013, 87(S2):S1-S2.

[91] Movsas B, Hu C, Sloan J, et al. Quality of life analysis of a radiation dose-escalation study of patients with non-small-cell lung cancer : a secondary analysis of the radiation therapy oncology group 0617 randomized clinical trial [J]. JAMA Oncol, 2016, 2(3):359-367.

[92] Bentzen SM, Parliament M, Deasy JO, et al. Biomarkers and surrogate endpoints for normal-tissue effects of radiation therapy : the importance of dose-volume effects [J]. Int J Radiat Oncol Biol Phys, 2010, 76(S3):S145-S150.

[93] Kong FM, Ten Haken RK, Schipper M, et al. Effect of midtreatment PET/CT-adapted radiation therapy with concurrent chemotherapy in patients with locally advanced non-small-cell lung cancer : a phase 2 clinical trial[J]. JAMA Oncol, 2017, 3(10):1358-1365.

[94] Schultheiss TE, Tome WA, Orton CG. Point/counterpoint : it is not appropriate to "deform" dose along with deformable image registration in adaptive radiotherapy [J]. Med Phys, 2012, 39(11):6531-6533.

[95] Liu F, Hu Y, Zhang Q, et al. Evaluation of deformable image registration and a motion model in CT images with limited features [J]. Phys Med Biol, 2012, 57(9):2539-2554.

[96] Burnet NG, Thomas SJ, Burton KE, et al. Defining the tumour and target volumes for radiotherapy [J]. Cancer imag, 2004, 4(2):153-161.

[97] Bentzen SM, Gregoire V. Molecular imaging-based dose painting : a novel paradigm for radiation therapy prescription [J]. Semin Radiat Oncol, 2011, 21(2):101-110.